

# Expression of *ATP-Binding Cassette Transporter A1 (ABCA1)* in Eyelid Tissues and Meibomian Gland Epithelial Cells

Fang Zheng,<sup>1,2</sup> Jingjing Su,<sup>2</sup> Jiaoman Wang,<sup>2</sup> Qing Zhan,<sup>2</sup> Mei Su,<sup>2</sup> Sicheng Ding,<sup>2</sup> Wei Li,<sup>3</sup> Ying-Ting Zhu,<sup>4</sup> and Ping Guo<sup>2</sup>

<sup>1</sup>Department of Ophthalmology, Jinzhou Medical University, Jinzhou, China

<sup>2</sup>Shenzhen Eye Institute, Shenzhen Eye Hospital, Jinan University, Shenzhen, China

<sup>3</sup>Eye Institute of Xiamen University, School of Medicine, Xiamen University, Xiamen, China

<sup>4</sup>BioTissue, Miami, Florida, United States

Correspondence: Ping Guo, Shenzhen Eye Institute, Shenzhen Eye Hospital, Jinan University, 18 Zetian Road, Futian District, Shenzhen, Guangdong 518040, China;

2607212858@qq.com.

Wei Li, Eye Institute of Xiamen University, School of Medicine, Xiamen University, South Xiang'an Rd., Xiamen, Fujian 361102, China; wei1018@xmu.edu.cn.

Ying-Ting Zhu, BioTissue, 7235 Corporate Center Drive, Suite B, Miami, FL 33126, USA; yzhu@biotissue.com.

FZ and JS contributed equally to the work presented here and should therefore be regarded as equivalent authors.

**Received:** November 5, 2023

**Accepted:** February 27, 2024

**Published:** March 19, 2024

Citation: Zheng F, Su J, Wang J, et al. Expression of *ATP-binding cassette transporter A1 (ABCA1)* in eyelid tissues and meibomian gland epithelial cells. *Invest Ophthalmol Vis Sci.* 2024;65(3):24. <https://doi.org/10.1167/iovs.65.3.24>

**PURPOSE.** To validate the *adenosine triphosphate (ATP)-binding cassette transporter A1 (ABCA1)* expression and distribution in human eyelid tissues and meibomian gland epithelial cells.

**METHODS.** Meibomian gland tissues from human eyelids were isolated by collagenase A digestion and cultured in defined keratinocyte serum-free medium (DKSFM). Infrared imaging was used to analyze the general morphology of meibomian glands. Hematoxylin and eosin (H&E) staining and Oil Red O staining were used to observe the morphological structure and lipid secretion in the human meibomian gland tissues. Quantitative real-time polymerase chain reaction, western blotting, and immunostaining were used to detect the mRNA and protein expression and cytolocalization of *ABCA1* in the meibomian gland tissues and cultured cells.

**RESULTS.** The degree of loss of human meibomian gland tissue was related to age. Meibomian gland lipid metabolism was also associated with age. Additionally, human meibomian gland tissues express *ABCA1* mRNA and protein; glandular epithelial cells express more *ABCA1* mRNA and protein than acinar cells, and their expression in acinar cells decreases with differentiation. Furthermore, the expression of *ABCA1* was downregulated in abnormal meibomian gland tissues. *ABCA1* was mainly localized on the cell membrane in primary human meibomian gland epithelial cells (pHMGEs), whereas it was localized in the cytoplasm of immortalized human meibomian gland epithelial cells (iHMGEs). The mRNA and protein levels of *ABCA1* in pHMGEs were higher than those in iHMGEs.

**CONCLUSIONS.** Meibomian gland tissues of the human eyelid degenerate with age. *ABCA1* expression in acinar cells decreases after differentiation and plays an important role in meibomian gland metabolism.

**Keywords:** *ABCA1*, meibomian gland, meibomian gland epithelial cells, lipid metabolism

Meibomian gland dysfunction (MGD) is the primary cause of evaporative dry eye syndrome,<sup>1,2</sup> accounting for >65% of dry eye cases,<sup>3</sup> with a global prevalence rate of 21.2% to 71.0%.<sup>4,5</sup> In China, the prevalence rate among people >40 years of age is 54.7% to 68.3%.<sup>6</sup> MGD is characterized by obstruction of the terminal ducts of the meibomian glands and/or changes in the quality or quantity of meibomian gland secretions.<sup>7</sup> Patients with moderate to severe MGD may develop ocular surface inflammation, and, in severe cases, complications such as corneal ulcers and perforation may occur, endangering visual function.<sup>8–10</sup> Lipid metabolism abnormalities may be an important factor in the occurrence and development of MGD.<sup>11–13</sup> With the rapid development of genomics, proteomics, and lipidomics,

the changes in gene expression of meibomian glands in patients with MGD and healthy individuals, as well as the differences and similarities in meibum proteins and lipid components, have become hot topics in this field. However, the mechanisms underlying meibum metabolism disorders and changes in meibum quality and quantity remain unclear.

The *adenosine triphosphate (ATP)-binding cassette transporter A1 (ABCA1)* gene is located on chromosome 9q31 and encodes a key rate-limiting protein in reverse cholesterol transport mediated by apolipoproteins.<sup>14,15</sup> *ABCA1* is widely found in the liver, gastrointestinal tract, adipose tissue, and macrophages, and it participates in cellular cholesterol homeostasis, regulation of cholesterol and phospholipid

content, and cell signaling transduction.<sup>16</sup> Therefore, the role of *ABCA1* in human metabolic diseases such as atherosclerosis, diabetes, Parkinson's disease, and Alzheimer's disease has become a popular research topic.<sup>17</sup>

*ABCA1* is expressed in the endothelial cells of Schlemm's canal, the optic nerve, and retinal tissues.<sup>18,19</sup> High *ABCA1* expression may promote lipid metabolism and clearance within retinal pigment epithelium (RPE) cells and reduce apoptosis thereof.<sup>20,21</sup> Inhibition of *ABCA1* and *scavenger receptor class B type I (SR-BI)* activity mediated by glibenclamide may eliminate the outflow of photoreceptor-derived lipids stimulated by high-density lipoproteins (HDLs) in cultured human RPE cells, supporting the role of reverse cholesterol transport regulation in the pathogenesis of age-related macular degeneration.<sup>22</sup> Nevertheless, it remains unclear whether *ABCA1* participates in the occurrence and development of MGD by regulating meibomian gland lipid metabolism.

Thus, identifying the expression and localization of *ABCA1* protein in human meibomian gland tissues and exploring the regulation of *ABCA1* in the physiological and pathological functions of meibomian glands would contribute to the clinical diagnosis and treatment of MGD. Therefore, we aimed to determine the expression and localization of *ABCA1* in ex vivo human meibomian gland tissues and in cultured meibomian gland epithelial cells, thus clarifying the expression intensity and localization of *ABCA1* in human meibomian gland tissues and cells and providing the possibility for further exploration of the role of *ABCA1* in meibomian gland metabolism.

## METHODS

### Reagents and Antibodies

Gibco Defined Keratinocyte Serum-Free Medium (DKSFM, 10744019); fetal bovine serum; penicillin–streptomycin; Gibco BASIC DMEM/F-12, HEPES (C11330500BT); Gibco Human EGF Recombinant Protein (PHG0311); Gibco Insulin–Transferrin–Selenium (ITS-G) (100×) (41400045); Gibco TrypLE Express Enzyme (1×), phenol red (12605010); Invitrogen *ABCA1* Polyclonal Antibody (PA1-16789); Invitrogen *PPAR gamma* Monoclonal Antibody (K.242.9) (MA5-14889); Invitrogen F(ab')<sub>2</sub>-Goat anti-Rabbit IgG (H+L) Cross-Adsorbed Secondary Antibody, Alexa Fluor Plus 488 (A48282TR); and Invitrogen Goat anti-Rabbit IgG (H+L) Secondary Antibody, HRP (31460) were all obtained from Thermo Fisher Scientific (Waltham, MA, USA). Hydrocortisone (M3451) was purchased from AbMole BioScience (Houston, TX, USA). The cell culture flasks and 6-, 12-, 24-, and 96-well culture plates were obtained from Corning (Corning, NY, USA).

### Human Eyelid Tissue Collection

Human eyelid tissues were obtained from the Shenzhen Eye Bank following the tenets of the Declaration of Helsinki, with the approval of the Ethics Committee of Shenzhen Eye Hospital and the Academic Committee of Ophthalmology in Shenzhen, China. All samples were obtained from the Shenzhen Red Cross Body Donation Reception Center, China, and informed consent forms for the use of the donated tissues were provided by the Center. All donors were of Han ethnicity, and tarsal plate tissues were obtained from human eyelids within 12 hours postmortem.

### Slit-Lamp Photography and Infrared Imaging of MGD Ex Vivo

After the skin, fibrous and connective tissues, muscles, and conjunctiva were removed from the human eyelid, the morphology of the tarsal gland was observed under a slit-lamp microscope. An OCULUS Keratograph 5M corneal topographer (OCULUS Optikgeräte GmbH, Wetzlar, Germany) was used to conduct infrared photography of the ex vivo tarsal gland by two professionals to evaluate the extent of glandular atrophy and absence (Fig. 1).

### Meibomian Gland Explant Culture

After infrared imaging, the ex vivo tarsal plate tissue was immersed in 0.5% iodophor (Adf, Shenzhen, China) for 2 minutes, followed by a 20-minute soak in a 1:2000 tobramycin working solution. The tissue was then cut into 2 × 2-mm pieces and digested with 2 mg/mL collagenase A at 37°C for 24 hours. Subsequently, the tissues were treated with Gibco Trypsin-EDTA (0.05%) for 5 to 8 minutes to form a single-cell suspension. The cells were then cultured in supplemental hormonal epithelial medium (SHEM) until they adhered to the wall, at which point the medium was switched to DKSFM containing 5 ng/mL epidermal growth factor (EGF) and 50 µg/mL bovine pituitary extract (BPE; M&C Gene Technology, Beijing, China). When the cell density reached 70% to 80%, a subculture was performed. The SHEM consisted of DMEM/F-12 supplemented with 5% fetal bovine serum, 1% penicillin–streptomycin, 1% ITS-G (100×), 0.5% dimethyl sulfoxide, 0.5-µg/mL hydrocortisone, and 10-ng/mL human EGF recombinant protein.<sup>23</sup> Immortalized human meibomian gland epithelial cells (iHMGECS), generously provided by David Sullivan, PhD, from Harvard Medical School,<sup>24</sup> were cultured in DKSFM supplemented with 5-ng/mL EGF and 50-µg/mL BPE. The cells were subcultured when they reached 70% to 80% confluence.<sup>25</sup>

### Histology

After infrared imaging of the meibomian glands, the central tarsal plate (three to five glands) was embedded in cryo-embedding matrix or paraffin and stored at –80°C (frozen sections) or 24°C to 26°C (paraffin sections). Paraffin sections were stained with hematoxylin and eosin (H&E), and frozen sections were subjected to immunofluorescence and Oil Red O staining.

### H&E Staining

All sections were obtained from the upper right eyelid. Sagittal sections (5 µm) were obtained using a microtome (HM525 NX Cryostat; Eppredia, Shanghai, China), with six sections per specimen stained with H&E and imaged using an optical microscope (BX43 Light Microscope; Olympus, Tokyo, Japan).

### Immunofluorescence

For meibomian gland immunostaining, frozen sections were fixed with 4% paraformaldehyde at room temperature, incubated with 0.2% Triton X-100, blocked with 2% BSA, incubated with the primary antibody overnight,

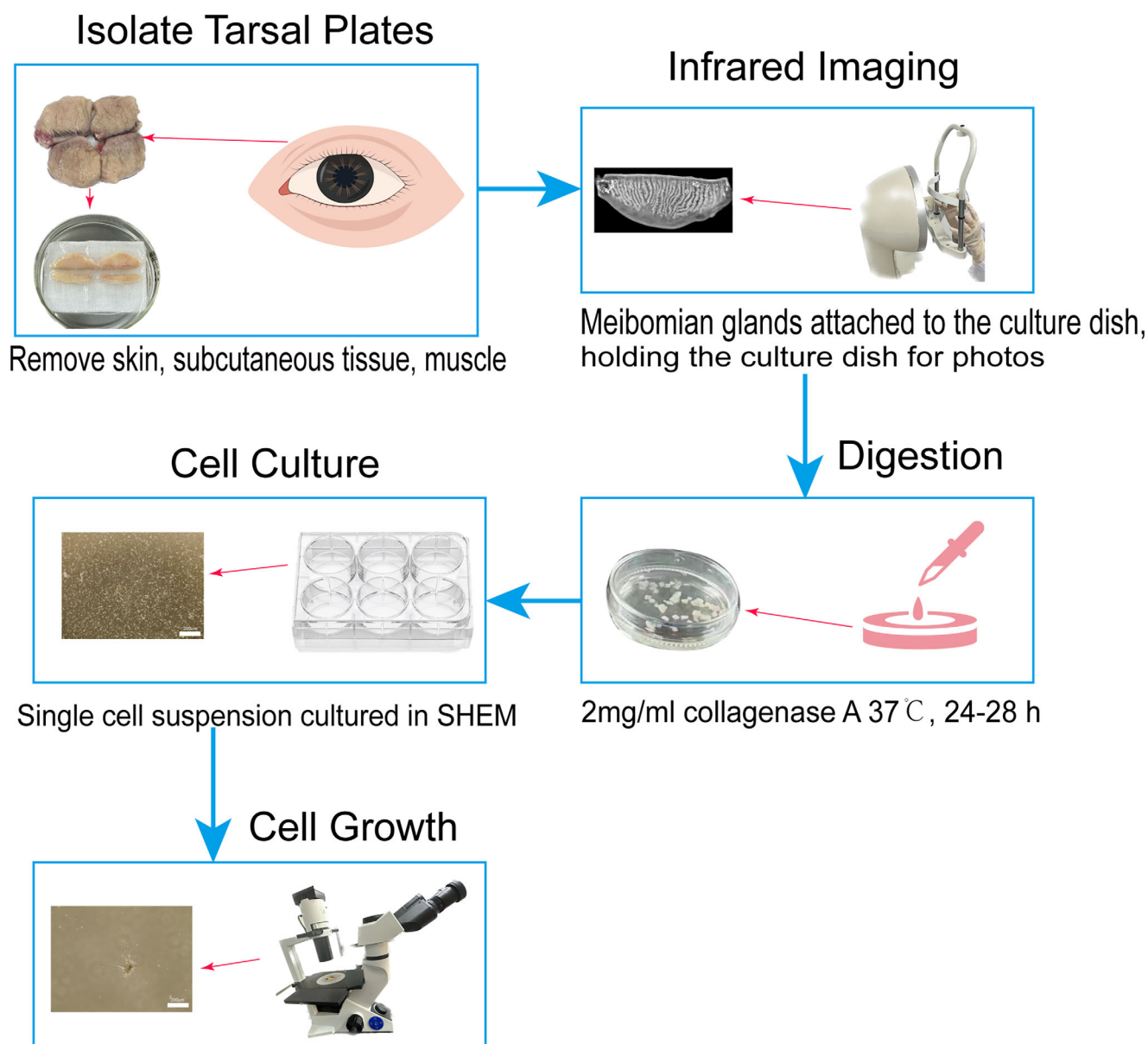


**FIGURE 1.** Infrared photography of human meibomian glands after separation and culture of primary meibomian gland epithelial cells.

washed, incubated with the secondary antibody, rinsed thoroughly, and observed under an inverted fluorescence microscope (Nikon Imaging, Tokyo, Japan) for image acquisition. Human meibomian gland epithelial cells were used for immunofluorescence staining. P2 cells in a 24-well culture plate were fixed with 4% paraformaldehyde after culture medium removal and thoroughly washed with phosphate-buffered saline (PBS). The remaining steps were the same as those used for tissue immunofluorescence staining.

#### Oil Red O Staining

Frozen meibomian gland sections were fixed in 4% paraformaldehyde solution for 10 minutes, washed with PBS for 5 minutes, and stained using the modified Oil Red O staining kit (Solarbio Life Science, Beijing, China). After being fixed, they were treated with buffer solution

for 2 to 5 minutes, stained with the staining solution for 15 minutes, differentiated with differentiation solution, and then rinsed with tap water to stop the differentiation and turn the cell nuclei blue. Finally, the sections were sealed with glycerin-gelatin and observed under an optical microscope.

#### RNA Extraction, Reverse Transcription, and Quantitative Real-Time Polymerase Chain Reaction

*ABCA1* mRNA was extracted from tissues or cells using an isolation kit (RE-03011; Foregene, Chengdu, China). After quantification using a NanoDrop Spectrophotometer (NanoDrop Technologies, Wilmington, DE, USA), cDNA was synthesized from 1 µg total RNA using the PrimeScript RT reagent kit (RR047A; Takara Bio, Shiga, Japan).

To quantify cDNA, real-time PCR was performed using the CFX96 Touch Real-Time PCR Detection System (Applied Biosystems, Waltham, MA, USA). The PCR amplification was conducted in a volume of 25  $\mu$ L using TB Green Premix Ex Taq II (RR802A; Takara BIO). The cycling protocol consisted of one cycle of 30 seconds at 95°C followed by 40 cycles at 95°C for 5 seconds and 60°C for 30 seconds. Subsequently, a melting curve analysis was conducted to confirm amplification specificity. Differential gene expression was calculated using the comparative threshold cycle method and normalized to *glyceraldehyde 3-phosphate dehydrogenase (GAPDH)* as the reference gene. The following primer sequences were used for amplification:

*ABCA1* forward primer: 5'-AGCAAGGAGCTGGCTGAAG-3'  
*ABCA1* reverse primer: 5'-GGTAGATTGGGTGGAGGA-3'  
*GAPDH* forward primer: 5'-AtCCCATCACCATCTTCC-3'  
*GAPDH* reverse primer: 5'-ATGACCCTTTTGGCTCCC-3'

### Western Blot Analysis

Meibomian gland samples and epithelial cell lysates were prepared using a radioimmunoprecipitation assay (RIPA) solution composed of protease and phosphatase inhibitors (BC3710; Solarbio Life Science), and protein concentrations were estimated using BCA (PC0020; Solarbio Life Science). Fifteen micrograms of protein from each sample were resolved on 4% to 12% precast polyacrylamide gels (F12412GEL; Changzhou Boyi Biotech Co., Ltd., Nanjing, China) under denaturing and reducing conditions for western blotting. The protein extracts were transferred to polyvinylidene difluoride membranes, which were then blocked with 5% fat-free milk in Tris-buffered saline containing 0.05% Tween 20 (T8220; Solarbio Life Science) at room temperature for 1 hour, followed by sequential incubation with a primary antibody for *ABCA1* (1:800) and a horseradish peroxidase-conjugated secondary antibody. *GAPDH* was used as a loading control. Protein signals were detected using an enhanced chemiluminescence reagent (1705060; Bio-Rad, Hercules, CA, USA) and an ultrasensitive multifunctional imager (Amersham Imager 680; GE Healthcare, Chicago, IL, USA).

### Statistical Analysis

Summary data are reported as mean  $\pm$  SD. Statistical comparisons among groups were performed through analysis of variance and Student's unpaired *t*-test using Prism 9.4 (GraphPad Software, Boston, MA, USA). Statistical significance was set at  $P < 0.05$ .

## RESULTS

### Human Meibomian Glands Show Degenerative Changes With Age

The loss of meibomian glands in donors increases with age. Meibomian gland tissues were obtained from 16 donors, including 12 men and FOUR women (age range, 12–90 years; average age,  $63.5 \pm 18.5$  years). Six cases corresponded to cerebrovascular accidents, four to malignant tumors, and five to chronic and congenital diseases; the remaining one was undefined (Table 1). Meibomian gland

loss grading from 0 to 3 by an experienced clinician based on infrared images yielded the following results: grade 0, eight cases (loss area, 0%–25%); grade 1, four cases (loss area, 26%–50%); grade 2, one case (loss area, 51%–75%); and grade 3, three cases (loss area, 76%–100%).<sup>26</sup> Given the small sample sizes, these observations require further investigation for accurate statistical analysis (Table 2).

The general morphology of human ex vivo meibomian glands was observed under a slit-lamp microscope (Fig. 2A). The meibomian gland tissues of adolescents were normal in shape, with moderate length and arrangement of the glands. The gland ducts and acini were visible under infrared light, with the acini arranged in a circular pattern around the gland. In middle-aged and elderly people, the clarity of the glands was significantly lower compared to younger people: approximately one-third of the glands in middle-aged people were atrophied, with shortened gland length and reduced acinar density. Central gland loss, twisting, and deformation were present in the elderly group (Fig. 2B).

### Lipid Metabolism Abnormalities Worsen With Age

H&E staining revealed significant differences in the acinar and ductal structures of the meibomian glands across different ages. In teenagers, lipid-producing acini could be seen entering the central duct obliquely through short branch tubules, with the acini being spherical or oval shaped and having a diameter of approximately 150 to 200  $\mu$ m. The duct was lined with a typical four-layer squamous epithelium, with basal cells being smaller and darker in color

TABLE 1. Donor Cause of Death and Slit-Lamp/Infrared Imaging Availability

Specimen	Age	Gender	Cause of Death	Infrared Imaging	Slit-Lamp Photography
1	50	M	CVA	✓	✓
2	53	M	CVA	✓	—
3	55	M	CVA	—	✓
4	72	F	CVA	✓	—
5	74	F	CVA	✓	✓
6	90	F	CVA	—	—
7	12	M	CCD	—	✓
8	68	M	CCD	—	✓
9	68	M	CCD	✓	—
10	68	M	CCD	✓	—
11	80	M	CCD	✓	✓
12	36	M	MT	✓	—
13	64	M	MT	✓	✓
14	70	M	MT	—	✓
15	73	M	MT	✓	—
16	83	F	Other	—	—

CCD, chronic and congenital disease; CVA, cardiovascular and cerebrovascular accident; F, female; M, male; MT, malignant tumor; ✓, images available.

TABLE 2. Grading of Meibomian Gland Loss

Grade	Number	Constituent Ratio
0	8	50%
1	4	25%
2	1	6%
3	3	19%
Total	16	100%



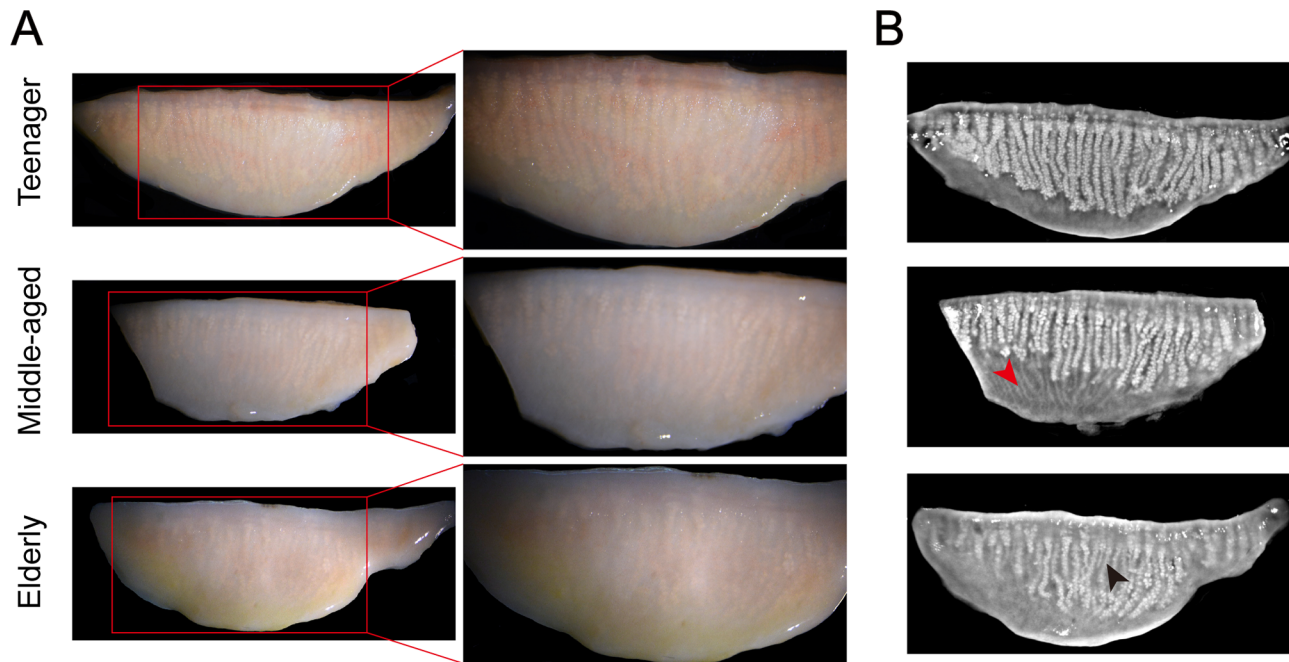


**FIGURE 2.** (A) Slit-lamp photography of the meibomian glands. (B) Infrared photography of the meibomian glands. The tarsal plates were separated from the cadaveric eyelids and divided into three age groups: teenager, middle-aged, and elderly. They were photographed directly after trimming some muscles and fascia. Note that the thickness of the tarsal plate and the setting of photographic lighting result in different transparencies. The two older donors (middle-aged and elderly) showed mild to moderate meibomian gland atrophy, accompanied by gland shortening (red arrow) or loss (black arrow).

compared to secretory cells (Fig. 3A). In contrast, in middle-aged individuals, the central duct was thickened due to an increase in epithelial cells. The duct was slightly dilated, and the atrophic acini were small and irregularly shaped. Compared with those of teenagers and middle-aged donors, the glandular structure of elderly donors showed significant changes, with gland shortening, central gland duct cystic expansion, thinner epithelium on the gland duct wall compared to normal glands, and some parts of the gland wall appearing wavy. The secretory acini were significantly smaller and rounder compared to those in normal glands, and the tubules were expanded and entered the central duct at a right angle. Atypical ducts formed within the acini, and the number of secretory cells decreased, leaving only a few cell layers.

Oil Red O staining revealed that lipid deposition increases with age. Compared to those of teenagers, the acini and ducts of middle-aged and elderly donors stained more prominently, especially in elderly donors, where the staining was strongly positive (Fig. 3B).

#### **ABCA1 Expression Is Downregulated in Abnormal Meibomian Gland Tissues**

Immunofluorescence and quantitative PCR (qPCR) were used to compare *ABCA1* expression in abnormal and normal meibomian gland tissues. The results showed strong staining for *ABCA1* in normal tissues but weak staining in abnormal tissues (Fig. 4). The staining in the meibomian gland duct epithelium was stronger than that in acinar cells. In basal acinar cells, *ABCA1* expression decreased as the degree of acinar epithelial cell differentiation increased. Quantitative real-time PCR (qRT-PCR) further confirmed that the gene

expression of *ABCA1* was reduced in the abnormal group ( $n = 6$ ,  $P < 0.05$ ). Although the samples might have contained pterygium tissue in addition to acinar ducts, this factor was unlikely to affect our detection of the difference in *ABCA1* expression between the abnormal and control groups, as *ABCA1* is not expressed in human meibomian connective tissues.

#### **Primary Culture of Human Meibomian Gland Cells**

Meibomian gland cells were successfully expanded using SHEM. After culturing the eyelid single-cell suspension in SHEM medium for 1 to 3 days, we observed oval or polygonal adherent cells, with fibroblast growth around adjacent cell colonies. After switching the medium to DKSFM, the cells showed logarithmic growth, and cell colonies began to form on the fifth day, with fibroblast growth inhibited, reaching 80% to 90% confluence in 10 to 12 days (Fig. 5). Beyond this confluence, the cells exhibited morphological aging (enlargement and flattening); cell growth slowed during P0, proliferation speed increased after P0, and cells at <P4 had a morphology similar to that of P0 cells. Subsequently, more cells became larger in volume, flatter, and more elongated, and the cell membrane began to break down.

#### **ABCA1 Expression in Human Primary Meibomian Gland Epithelial Cells and Immortalized Cells**

*Peroxisome proliferator-activated receptor gamma (PPAR-γ)* is a crucial regulator of adipogenesis and adipocyte differentiation,<sup>27</sup> and studies have shown that changes in *PPAR-γ* receptor signaling in aged mice may lead to corresponding changes in lipid synthesis and glandular atrophy.<sup>28</sup> If *PPAR-γ*

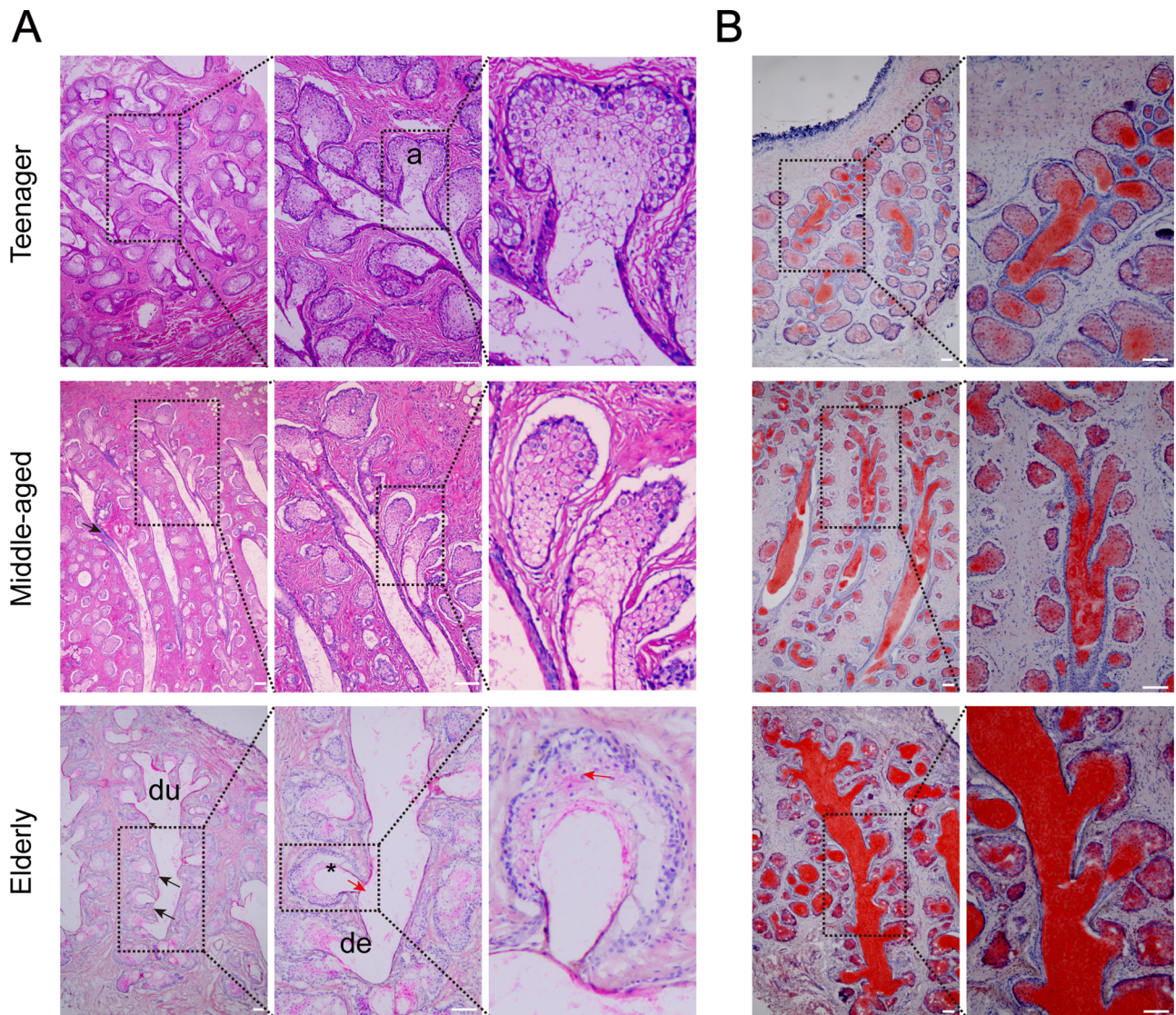


**FIGURE 3.** Human meibomian gland structure and lipid metabolism performance. **(A)** H&E staining of meibomian gland ducts and acini ( $n = 3$ ). Abbreviations: a, acini; du, central duct; de, connecting ductule. **(B)** Oil Red O staining of meibomian glands ( $n = 3$ ). Scale bar: 100  $\mu$ m.

expression is lost, lipid production may decrease, leading to age-related MGD.<sup>29</sup> As meibomian gland cells lack specific protein markers, we used *PPAR- $\gamma$*  and Nile Red to identify the cells (Fig. 6). Subsequently, ABCA1-specific antibodies were used to immunostain P2 cultures and iHMGEs. The results showed that ABCA1 was mainly expressed on the cell membrane of primary human meibomian gland epithelial cells (pHMGEs), but this localization was not detected in iHMGEs using the same antibody. Proteins extracted from the cultured cells showed that the expression in pHMGEs was significantly higher than that in iHMGEs. Additionally, when ABCA1 transcript levels were measured in the two cell lines, the expression in pHMGEs was 1.2 times higher than that in iHMGEs, which is inconsistent with the report by Liu et al.,<sup>24</sup> who have shown essentially no difference in mRNA expression between these cell preparations. This discrepancy might have its origin in the differences in cell culture procedure and environment, such as co-culture with 3T3 layer at first (theirs) versus no co-culture (ours);

culture medium composition with different EGF concentrations (theirs, 2.5  $\mu$ g/mL; ours, 10 ng/mL); with the cholera toxin A subunit (theirs) or without (ours); and different FBS concentrations (theirs, 10%; ours, 5%). Our results indicate that both pHMGEs and iHMGEs express ABCA1 and that ABCA1 mRNA and protein levels in pHMGEs are higher than those in iHMGEs.

## DISCUSSION

Our study yielded two key findings. First, human meibomian gland tissues express ABCA1, with higher expression in ductal epithelial cells than in acinar cells, and acinar expression decreases as the acini differentiate. Second, the expression level of ABCA1 in abnormal meibomian glands is lower than that in the control group (normal meibomian glands). However, this phenomenon was not verified by western blotting and requires further investigation.



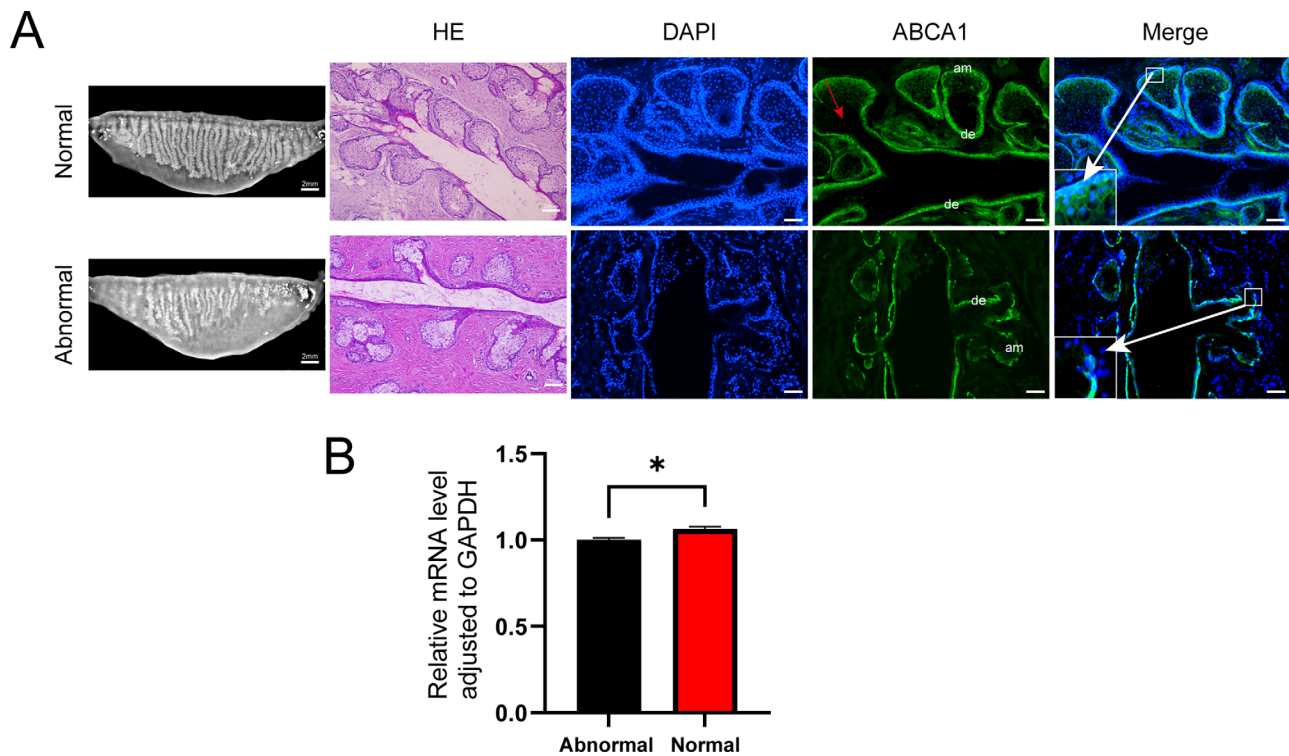


**FIGURE 4.** Localization and expression of *ABCA1* in the meibomian gland. (A) Immunofluorescence staining showed reduced expression of *ABCA1* in abnormal meibomian glands. Compared to other eyelid tissues, *ABCA1* staining was strong in meibomian gland duct epithelium, acinar basal cells, and progenitor cells. In acinar cells, nuclear colocalization (DAPI) showed that the intensity of *ABCA1* expression decreased as the degree of cell differentiation increased (direction of red arrow). (B) qPCR results showed that *ABCA1* mRNA levels were higher in the normal meibomian gland function group compared to the abnormal meibomian gland function group ( $P < 0.05$ ,  $n = 3$ ).

Meibomian gland atrophy and dropout are the most important pathological features of MGD.<sup>30</sup> Although the mechanism of atrophy is unclear, age and blockage of the eyelid gland opening are the main risk factors. It is also unclear how the atrophy caused by these two factors differs. Meibomian gland atrophy progresses with increasing age, and human meibomian gland atrophy may be detected as early as at 25 years of age and continues to develop after 60 years of age, manifesting as morphological and functional changes that include progressive gland dropout and reduced meibum secretion.<sup>31–33</sup> Arita et al.<sup>34</sup> reported that gland dropout in men begins at 20 years of age in men and 30 years of age in women. Analysis of these changes shows that individuals over 50 have significantly more gland dropout than younger people. However, no difference was found among individuals 51 to 60 years of age and those over 60.<sup>35,36</sup> Various morphological characteristics of abnormal eyelid glands exist in healthy individuals. With aging, only moderate-to-severe short glands show an increase in abnormal morphological characteristics. Our results confirm and extend these early findings. With aging, the acini of the elderly differed from normal round acini, exhibiting atrophy, smaller volume, and irregular shape. Additionally, acinar lipid production was reduced: from many small lipid droplets in young individuals to fewer and larger lipid droplets in older individuals. A phenomenon of lipid concentration and accumulation in the eyelid glands of older individuals indicates abnormal lipid metabolism in the eyelid glands.

The meibomian gland is a tubuloacinar sebaceous gland that synthesizes and secretes meibum. The force is gener-

ated by the contraction of the orbicularis oculi and Riolan's muscles, and closure of the eyelid during blinking evenly distributes the meibum ester to the surface of the tear film, forming its lipid layer.<sup>37,38</sup> Meibum is composed of a complex mixture of lipids. The majority are nonpolar, including wax esters (WEs), cholesteryl esters (CEs), free cholesterol, fatty acids, and triglycerides, whereas a minority of them are polar, including phospholipids, sphingolipids, and glycolipids.<sup>39</sup> MGD can cause changes in the lipid composition of meibomian gland secretions. Abnormal lipids may lead to irregularities in the composition and function of the tear film and are the main cause of evaporative dry eye disease.<sup>31,40</sup> The process of lipid metabolism contributes to the development of many chronic and inflammatory diseases; therefore, understanding lipid metabolism complexity is crucial for medical interventions in the MGD population. Systematic changes in lipid metabolism have been extensively studied.<sup>41–43</sup> Recently, Nagar et al.<sup>44</sup> showed that, as MGD severity increases, the molar ratios of CE to WE ( $R_{CE/WE}$ ) in peripheral blood gradually decrease. This indicates a connection between  $R_{CE/WE}$  in the meibum and MGD severity. An increase in the ratio of aldehyde to wax ester ( $R_{ald/WE}$ ) in meibum is considered a potential marker of MGD severity. Additionally, from the comparative lipidomic analysis on the tarsal plate, a significant similarity has been noted between mouse and human samples.<sup>45</sup> Several age-related lipid molecules and protein biomarkers from the cholesterol biosynthesis pathway may be involved in MGD onset.<sup>13</sup> Common and age-related MGD are closely related to abnormal lipid metabolism.

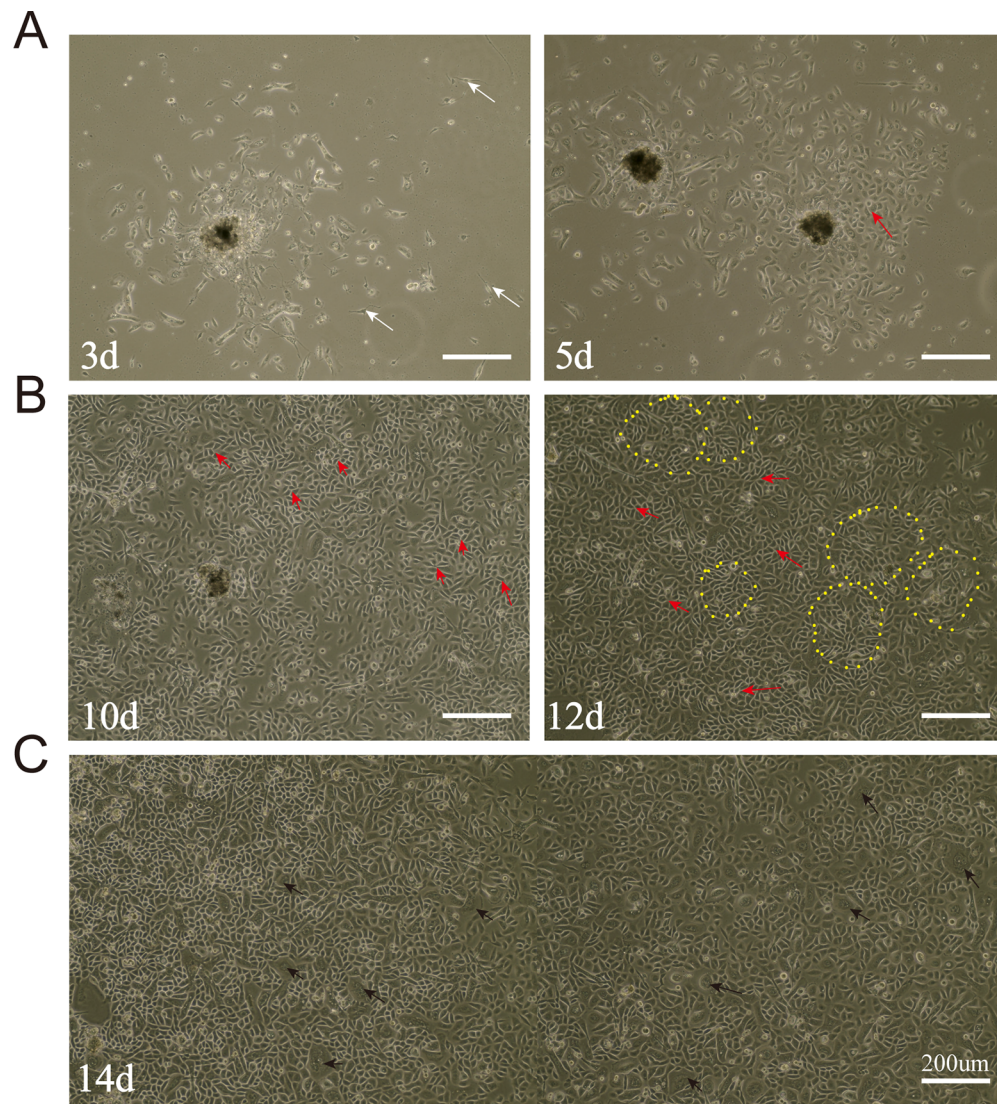


**FIGURE 5.** Representative images of human P0 primary eyelid gland epithelial cells under an inverted microscope. (A) Human eyelid gland cultured ex vivo at day 3 and day 5. Fibroblast growth was seen around the glands (*white arrows*). (B) On days 10 to 12, cells fused to form many cell clusters (*red arrows* and *yellow circles*), with a confluence rate of 80%–90%. (C) After achieving a confluence of more than 90%, the cells became flat and enlarged, showing signs of cellular aging (*black arrows*).

*ABCA1* regulates various key cellular functions, such as phagocytosis, inflammation, intracellular signaling, cell proliferation, and apoptosis.<sup>17</sup> The function of *ABCA1* was determined from research on Tangier disease, in which patients exhibit hypercholesterolemia due to the lack of *ABCA1*, with clinical symptoms including orange-yellow tonsil hypertrophy, hepatosplenomegaly, neuropathy, corneal opacity, thrombocytopenia, anemia, and stomatocytosis.<sup>46–48</sup> There are no reports on the meibomian gland phenotype in Tangier disease.

*ABCA1* is widely distributed in various tissues and organs of the human body and may transport cholesterol and phospholipids to *apolipoprotein A-I* (*apoA-I*), *apolipoprotein E* (*apoE*), or other apolipoproteins, thus regulating the synthesis of HDL and the reverse transport of cholesterol, as well as playing an important role in maintaining the stability of lipid metabolism in the body.<sup>49,50</sup> The expression level and functional abnormalities of *ABCA1* are related to the occurrence and development of some metabolic, cardiovas-

cular, and nervous system diseases.<sup>16</sup> Importantly, Chen et al.<sup>51</sup> utilized qRT-PCR to confirm that *ABCA1* is extensively expressed in ocular tissues such as the human trabecular meshwork, Schlemm's canal endothelial cells, optic nerve, and retina. Several studies have measured the expression of *ABCA1* in ocular surface tissues.<sup>24,37,52,53</sup> Differences in *ABCA1* expression were noted in the meibomian glands of mice following testosterone therapy.<sup>54</sup> In addition, treatment of iHMGECs with EGF and/or BPE to induce proliferation significantly altered the transcription level of *ABCA1* and other lipid metabolism-related genes.<sup>55</sup> Despite some reports on *ABCA1* expression in ocular surface tissues, no reports have been noted on the specific localization of *ABCA1* or function studies in human eyelid tissues. To our knowledge, this is the first study to report strong *ABCA1* expression in human meibomian gland acinar cells and HMGECs. Moreover, as meibocytes differentiate, *ABCA1* expression tends to diminish, and the expression of *ABCA1* is downregulated in abnormal meibomian gland tissues.



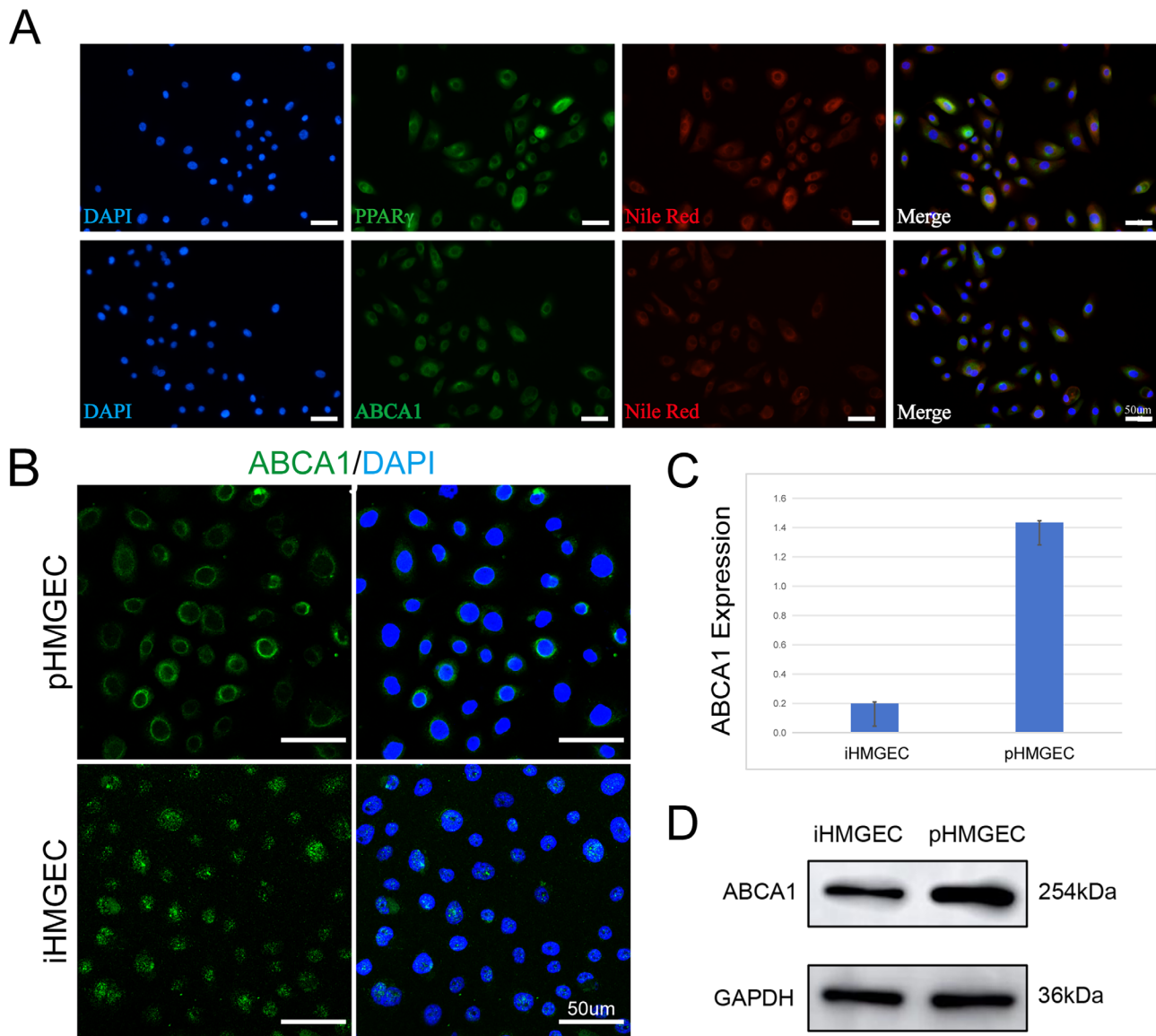


**FIGURE 6.** Expression and cytolocation of *ABCA1* in meibomian gland epithelial cells in culture. **(A)** *PPAR-γ* (green), *ABCA1* (green), Nile Red (red), and cell nucleus DAPI (blue) staining in P2 pHMGECs. **(B)** Immunofluorescence staining showed that *ABCA1* was mainly expressed on the cell membrane in pHMGECs rather than in the cytoplasm in iHMGECS. **(C)** qRT-PCR showed that the expression of *ABCA1* mRNA in pHMGECs was higher than that in iHMGECS. **(D)** Western blot analysis of *ABCA1* in pHMGECs and iHMGECS.

Interestingly, we have also noted that the *ABCA1* expression level in pHMGECs was higher than that in iHMGECS in our model. Based on these findings, we believe that *ABCA1* may play a significant role in regulating lipid metabolism in meibomian glands, mediating meibocyte physiological functions such as differentiation. Furthermore, the *liver X receptor* (*LXR*) agonist TO901317 ameliorates  $\beta$ -amyloid protein-induced retinal inflammation by suppressing *nuclear factor kappa B* (*NF-κB*) signal transduction and NLRP3 inflammasome activation, thereby activating the *LXRα-ABCA1* axis. *LXRα* and *LXRβ* upregulate the expression of *ABCA1*, which enhances lipid metabolism and clearance in retinal pigment epithelial cells and reduces apoptosis.<sup>20</sup> Furthermore, impaired lipid efflux mediated by *ABCA1/ABCG1* in mouse RPE may lead to retinal degeneration.<sup>56</sup> *ABCA1* is capable of regulating intraocular pressure by adjusting the Cav1/eNOS/NO signaling pathway.<sup>57</sup>

To understand the regulation of meibum metabolism and synthesis, Liu et al.<sup>24</sup> established an immortalized human meibomian gland epithelial cell line in 2010, and iHMGECS have been used as a model to study MGD physiology and pathophysiology in vitro. *Acyl-CoA wax-alcohol acyltransferase 2* (*AWAT2*), a key gene required for normal meibomian gland synthesis, is absent in iHMGECS.<sup>58</sup> In addition, WE and CE are considered to be the main components of meibum. Furthermore, lipidomic analysis has shown that the CE content in serum-treated iHMGECS is approximately 5%, whereas that of WE is less than 1%. In iHMGECS, the levels of these two types of lipids have been found to be significantly lower than the normal level, suggesting that these cells were abnormal in their culture conditions.<sup>59</sup> Sullivan et al.<sup>60</sup> reported that the iHMGECS lipid composition does not mirror the levels of neutral and polar lipids usually present in human meibum. The authors spec-

ulated that this might be because the ductal cells—like those in other exocrine glands, could alter the composition of their luminal secretions. Interestingly, Thiboutot<sup>61</sup> hypothesized that phospholipids are recycled within sebaceous gland ducts following overall secretion, leading to the primary transport of neutral lipids to the skin. This recycling process may also occur in meibomian glands, which could explain, for example, why meibum lacks phospholipids. Finally, there are only three records of pHMGECs. The most recent one was reported by Duong et al.,<sup>62</sup> who used cells cultured from biopsy-sized human eyelid tissues obtained during ocular plastic surgery; transcriptomic analysis confirmed high-level expression of genes related to cell origin and lipogenesis. We have outlined a different, detailed method for pHMGEC culture, with single-cell suspensions first adhering in SHEM before being switched to DKSFM to promote cell proliferation. This method successfully established primary cultures of human meibomian gland cells from cadaveric eyelid tissue. We showed that *ABCA1* is primarily expressed on the cell membrane of pHMGECs, whereas it does not exhibit the same pattern in iHMGECs, in which it is primarily located in the cytoplasm. Moreover, qRT-PCR and western blot results showed that the transcript and protein levels of *ABCA1* were higher in pHMGECs compared to iHMGECs, perhaps because the cells exhibit different phenotypes under different culture conditions. In future studies, a comparative investigation will be conducted using pHMGEC and iHMGEC lines under different culture conditions to determine the best model to study MGD pathophysiology.

It is necessary to acknowledge the limitations of this study. First, due to uncontrollable factors related to human tissue donation, the availability of human eyelid tissues was limited, and there were no clear selection criteria or age ranges for tissue collection, which might have affected the accuracy of our results. In addition, *ABCA1* expression may be altered by tissue freshness. Eyelid tissues were collected from our eye bank within 12 hours of death. In the future, we will use a larger sample size to confirm our results, and we are planning to validate our research on animal and in vitro models.

In summary, the age-related regressive changes observed in human meibomian glands are consistent with those reported in previous studies. *ABCA1* is expressed in both meibomian gland tissues and in vitro cultured acinar cells. Thus, our results provide a new direction for research into the pathophysiology of MGD; that is, *ABCA1* may be involved in acinar cell differentiation and lipid synthesis. Moving forward, we aim to further investigate the role of *ABCA1* in meibomian glands using HMGECS and MGD animal models.

### Acknowledgments

The authors thank the Shenzhen Eye Bank for providing the human eyelid tissues. We also thank Yuli Guo and Rongrong Zhang from Xiamen University Eye Institute, China for their help with cell culture.

Supported by the Science, Technology, and Innovation Commission of Shenzhen Municipality (JCYJ20230807114605011).

Disclosure: **F. Zheng**, None; **J. Su**, None; **J. Wang**, None; **Q. Zhan**, None; **M. Su**, None; **S. Ding**, None; **W. Li**, None; **Y.-T. Zhu**, None; **P. Guo**, None

### References

1. Paranjpe V, Galor A, Gramberg R, Mandal N. The role of sphingolipids in meibomian gland dysfunction and ocular surface inflammation. *Ocul Surf*. 2022;26:100–110.
2. Sabeti S, Kheirkhah A, Yin J, Dana R. Management of meibomian gland dysfunction: a review. *Surv Ophthalmol*. 2020;65:205–217.
3. Alghamdi YA, Mercado C, McClellan AL, Batawi H, Karp CL, Galor A. Epidemiology of meibomian gland dysfunction in an elderly population. *Cornea*. 2016;35:731–735.
4. Hassanzadeh S, Varmaghani M, Zarei-Ghanavati S, Heravian Shandiz J, Azimi Khorasani A. Global prevalence of meibomian gland dysfunction: a systematic review and meta-analysis. *Ocul Immunol Inflamm*. 2021;29:66–75.
5. McCann P, Abraham AG, Mukhopadhyay A, et al. Prevalence and incidence of dry eye and meibomian gland dysfunction in the United States: a systematic review and meta-analysis. *JAMA Ophthalmol*. 2022;140:1181–1192.
6. Jie Y, Xu L, Wu YY, Jonas JB. Prevalence of dry eye among adult Chinese in the Beijing Eye Study. *Eye (Lond)*. 2009;23:688–693.
7. Du YL, Peng X, Liu Y, et al. Ductal hyperkeratinization and acinar renewal abnormality: new concepts on pathogenesis of meibomian gland dysfunction. *Curr Issues Mol Biol*. 2023;45:1889–1901.
8. Nelson JD, Shimazaki J, Benitez-del-Castillo JM, et al. The International Workshop on Meibomian Gland Dysfunction: report of the definition and classification subcommittee. *Invest Ophthalmol Vis Sci*. 2011;52:1930–1937.
9. Chhadva P, Goldhardt R, Galor A. Meibomian gland disease: the role of gland dysfunction in dry eye disease. *Ophthalmology*. 2017;124:S20–S26.
10. Corrales RM, Stern ME, De Paiva CS, Welch J, Li DQ, Pflugfelder SC. Desiccating stress stimulates expression of matrix metalloproteinases by the corneal epithelium. *Invest Ophthalmol Vis Sci*. 2006;47:3293–3302.
11. Bu J, Zhang M, Wu Y, et al. High-fat diet induces inflammation of meibomian gland. *Invest Ophthalmol Vis Sci*. 2021;62:13.
12. Yoo YS, Park SK, Hwang HS, Kim HS, Arita R, Na KS. Association of serum lipid level with meibum biosynthesis and meibomian gland dysfunction: a review. *J Clin Med*. 2022;11:4010.
13. Cai Y, Zhang S, Chen L, Fu Y. Integrated multi-omics and machine learning approach reveals lipid metabolic biomarkers and signaling in age-related meibomian gland dysfunction. *Comput Struct Biotechnol*. 2023;21:4215–4227.
14. Wang J, Xiao Q, Wang L, Wang Y, Wang D, Ding H. Role of *ABCA1* in cardiovascular disease. *J Pers Med*. 2022;12:1010.
15. Puntoni M, Sbrana F, Bigazzi F, Sampietro T. Tangier disease: epidemiology, pathophysiology, and management. *Am J Cardiovasc Drugs*. 2012;12:303–311.
16. Jacobo-Albavera L, Domínguez-Pérez M, Medina-Leyte DJ, González-Garrido A, Villarreal-Molina T. The role of the ATP-binding cassette A1 (ABCA1) in human disease. *Int J Mol Sci*. 2021;22:1593.
17. Paseban T, Alavi MS, Etemad L, Roohbakhsh A. The role of the ATP-binding cassette A1 (ABCA1) in neurological disorders: a mechanistic review. *Expert Opin Ther Targets*. 2023;27:531–552.
18. Gharahkhani P, Burdon KP, Fogarty R, et al. Common variants near *ABCA1*, *AFAP1* and *GMDS* confer risk of primary open-angle glaucoma. *Nat Genet*. 2014;46:1120–1125.
19. Cai J, Perkumas KM, Qin X, Hauser MA, Stamer WD, Liu Y. Expression profiling of human Schlemm's canal endothelial cells from eyes with and without glaucoma. *Invest Ophthalmol Vis Sci*. 2015;56:6747–6753.

20. Lei C, Lin R, Wang J, et al. Amelioration of amyloid  $\beta$ -induced retinal inflammatory responses by a LXR agonist TO901317 is associated with inhibition of the NF- $\kappa$ B signaling and NLRP3 inflammasome. *Neuroscience*. 2017;360:48–60.
21. Storti F, Raphael G, Griesser V, et al. Regulated efflux of photoreceptor outer segment-derived cholesterol by human RPE cells. *Exp Eye Res*. 2017;165:65–77.
22. Duncan KG, Bailey KR, Kane JP, Schwartz DM. Human retinal pigment epithelial cells express scavenger receptors BI and BII. *Biochem Biophys Res Commun*. 2002;292:1017–1022.
23. Solomon A, Rosenblatt M, Monroy D, Ji Z, Pflugfelder SC, Tseng SC. Suppression of interleukin  $1\alpha$  and interleukin  $1\beta$  in human limbal epithelial cells cultured on the amniotic membrane stromal matrix. *Br J Ophthalmol*. 2001;85:444–449.
24. Liu S, Hatton MP, Khandelwal P, Sullivan DA. Culture, immortalization, and characterization of human meibomian gland epithelial cells. *Invest Ophthalmol Vis Sci*. 2010;51:3993–4005.
25. Liu R, Li J, Xu Y, et al. Melatonin attenuates LPS-induced proinflammatory cytokine response and lipogenesis in human meibomian gland epithelial cells via MAPK/NF- $\kappa$ B pathway. *Invest Ophthalmol Vis Sci*. 2022;63:6.
26. Adil MY, Xiao J, Olafsson J, et al. Meibomian gland morphology is a sensitive early indicator of meibomian gland dysfunction. *Am J Ophthalmol*. 2019;200:16–25.
27. Guo Y, Zhang H, Zhao Z, et al. Hyperglycemia induces meibomian gland dysfunction. *Invest Ophthalmol Vis Sci*. 2022;63:30.
28. Kim SW, Xie Y, Nguyen PQ, et al. PPAR $\gamma$  regulates meibocyte differentiation and lipid synthesis of cultured human meibomian gland epithelial cells (hMGEC). *Ocul Surf*. 2018;16:463–469.
29. Jester JV, Potma E, Brown DJ. PPAR $\gamma$  regulates mouse meibocyte differentiation and lipid synthesis. *Ocul Surf*. 2016;14:484–494.
30. Tomlinson A, Bron AJ, Korb DR, et al. The International Workshop on Meibomian Gland Dysfunction: report of the Diagnosis Subcommittee. *Invest Ophthalmol Vis Sci*. 2011;52:2006–2049.
31. Yang X, Reneker LW, Zhong X, Huang AJW, Jester JV. Meibomian gland stem/progenitor cells: the hunt for gland renewal. *Ocul Surf*. 2023;29:497–507.
32. Villani E, Canton V, Magnani F, Viola F, Nucci P, Ratiglia R. The aging Meibomian gland: an in vivo confocal study. *Invest Ophthalmol Vis Sci*. 2013;54:4735–4740.
33. Yeotikar NS, Zhu H, Markoulli M, Nichols KK, Naduvilath T, Papas EB. Functional and morphologic changes of meibomian glands in an asymptomatic adult population. *Invest Ophthalmol Vis Sci*. 2016;57:3996–4007.
34. Arita R, Itoh K, Inoue K, Amano S. Noncontact infrared meibography to document age-related changes of the meibomian glands in a normal population. *Ophthalmology*. 2008;115:911–915.
35. Pult H, Riede-Pult BH, Nichols JJ. Relation between upper and lower lids' meibomian gland morphology, tear film, and dry eye. *Optom Vis Sci*. 2012;89:E310–E315.
36. Kim HM, Eom Y, Song JS. The relationship between morphology and function of the meibomian glands. *Eye Contact Lens*. 2018;44:1–5.
37. Knop E, Knop N, Millar T, Obata H, Sullivan DA. The International Workshop on Meibomian Gland Dysfunction: report of the Subcommittee on Anatomy, Physiology, and Pathophysiology of the Meibomian Gland. *Invest Ophthalmol Vis Sci*. 2011;52:1938–1978.
38. Yokoi N, Komuro A. Non-invasive methods of assessing the tear film. *Exp Eye Res*. 2004;78:399–407.
39. Butovich IA. Meibomian glands, meibum, and meibogenesis. *Exp Eye Res*. 2017;163:2–16.
40. Borchman D, Ramasubramanian A, Foulks GN. Human meibum cholesteryl and wax ester variability with age, sex, and meibomian gland dysfunction. *Invest Ophthalmol Vis Sci*. 2019;60:2286–2293.
41. Jun I, Kim BR, Park SY, et al. Interleukin-4 stimulates lipogenesis in meibocytes by activating the STAT6/PPAR $\gamma$  signaling pathway. *Ocul Surf*. 2020;18:575–582.
42. Kam WR, Liu Y, Ding J, Sullivan DA. Do cyclosporine A, an IL-1 receptor antagonist, uridine triphosphate, rebamipide, and/or bimatoprost regulate human meibomian gland epithelial cells? *Invest Ophthalmol Vis Sci*. 2016;57:4287–4294.
43. Yoon CH, Ryu JS, Ko JH, et al. The eyelid meibomian gland deficiency in fucosyltransferase 1 knockout mice. *Int J Mol Sci*. 2022;23:9464.
44. Nagar S, Ajouz L, Nichols KK, et al. Relationship between human meibum lipid composition and the severity of meibomian gland dysfunction: a spectroscopic analysis. *Invest Ophthalmol Vis Sci*. 2023;64:22.
45. Butovich IA, McMahon A, Wojtowicz JC, Lin F, Mancini R, Itani K. Dissecting lipid metabolism in meibomian glands of humans and mice: an integrative study reveals a network of metabolic reactions not duplicated in other tissues. *Biochim Biophys Acta*. 2016;1861:538–553.
46. Kocen RS. Tangier disease. *J Neurol Neurosurg Psychiatry*. 2004;75:1368.
47. Hooper AJ, Hegele RA, Burnett JR. Tangier disease: update for 2020. *Curr Opin Lipidol*. 2020;31:80–84.
48. Koseki M, Yamashita S, Ogura M, et al. Current diagnosis and management of Tangier disease. *J Atheroscler Thromb*. 2021;28:802–810.
49. Marchi C, Adorni MP, Caffarra P, et al. ABCA1- and ABCG1-mediated cholesterol efflux capacity of cerebrospinal fluid is impaired in Alzheimer's disease. *J Lipid Res*. 2019;60:1449–1456.
50. Karasinska JM, de Haan W, Franciosi S, et al. ABCA1 influences neuroinflammation and neuronal death. *Neurobiol Dis*. 2013;54:445–455.
51. Chen Y, Lin Y, Vithana EN, et al. Common variants near ABCA1 and in PMM2 are associated with primary open-angle glaucoma. *Nat Genet*. 2014;46:1115–1119.
52. Liu S, Richards SM, Lo K, Hatton M, Fay A, Sullivan DA. Changes in gene expression in human meibomian gland dysfunction. *Invest Ophthalmol Vis Sci*. 2011;52:2727–2740.
53. Ziemanski JF, Chen J, Nichols KK. Evaluation of cell harvesting techniques to optimize lipidomic analysis from human meibomian gland epithelial cells in culture. *Int J Mol Sci*. 2020;21:3277.
54. Schirra F, Suzuki T, Richards SM, et al. Androgen control of gene expression in the mouse meibomian gland. *Invest Ophthalmol Vis Sci*. 2005;46:3666–3675.
55. Liu S, Kam WR, Ding J, Hatton MP, Sullivan DA. Effect of growth factors on the proliferation and gene expression of human meibomian gland epithelial cells. *Invest Ophthalmol Vis Sci*. 2013;54:2541–2550.
56. Storti F, Klee K, Todorova V, et al. Impaired ABCA1/ABCG1-mediated lipid efflux in the mouse retinal pigment epithelium (RPE) leads to retinal degeneration. *eLife*. 2019;8:e45100.
57. Hu C, Niu L, Li L, et al. ABCA1 regulates IOP by modulating Cav1/eNOS/NO signaling pathway. *Invest Ophthalmol Vis Sci*. 2020;61:33.

58. Rho CR, Kim SW, Lane S, et al. Expression of Acyl-CoA wax-alcohol acyltransferase 2 (AWAT2) by human and rabbit meibomian glands and meibocytes. *Ocul Surf.* 2022;23:60–70.
59. Hampel U, Schröder A, Mitchell T, et al. Serum-induced keratinization processes in an immortalized human meibomian gland epithelial cell line. *PLoS One.* 2015;10: e0128096.
60. Sullivan DA, Liu Y, Kam WR, et al. Serum-induced differentiation of human meibomian gland epithelial cells. *Invest Ophthalmol Vis Sci.* 2014;55:3866–3877.
61. Thiboutot D. Regulation of human sebaceous glands. *J Invest Dermatol.* 2004;123:1–12.
62. Duong HT, Phan MAT, Madigan MC, et al. Culture of primary human meibomian gland cells from surgically excised eyelid tissue. *Exp Eye Res.* 2023;235:109636.